THE JOURNAL OF PHYSICAL CHEMISTRY C

ARTICLE

pubs.acs.org/JPCC

Mechanism of Oxygen Electro-Reduction on Au-Modified Pt: Minimizing O Coverage and Pt Site Exposure toward Highly Stable and Active Cathode

Ya-Hui Fang and Zhi-Pan Liu*

Shanghai Key Laboratory of Molecular Catalysis and Innovative Materials, Department of Chemistry, Key Laboratory of Computational Physical Science (Ministry of Education), Fudan University, Shanghai 200433, China

Supporting Information

ABSTRACT: To catalyze oxygen reduction reaction (ORR) under electrochemical conditions approaching its thermodynamic limit, i.e., 1.23 V vs NHE, has been consistently pursued by chemists. It is known that metal electrodes, even noble metals, undergo severe corrosion at the high potential, accompanied with the rapid decrease in activity. A comprehensive understanding of both the stability and the catalytic activity of the Pt surface is urgently called for toward the rational design of a new ORR catalyst. This work, by utilizing chemically inert Au as a modifier to the Pt surface, investigated the stability and the activity of a set of Au/Pt composites using first-principles-based theoretical methods designed for the modeling of solid/liquid electrocatalysis. By computing the surface phase diagram and the corrosion thermodynamics, we demonstrate that the presence of Au can remarkably reduce the in situ O atom coverage to be below a critical local 0.5 monolayer (ML) and thus protect the neighboring Pt sites from corrosion. The AuPt surface alloy with a very low amount of Au dispersing in the Pt surface layer is sufficient to stabilize the whole catalyst surface. With the calculated ORR profiles, we show that ORR activity in AuPt surface alloys is not sensitive to the Au concentration, and a good activity is maintained with the Au concentration up to 7/8 ML. Fundamentally, this is because the minimum active site of ORR requires only two neighboring Pt atoms (with an OOH pathway), and the majority of surface Pt sites on pure Pt are in fact nonactive spectators that are terminated by O atoms at the working potentials. The key factors controlling the ORR activity and surface stability are therefore unified as *the minimum O coverage and the minimum exposure of Pt (active) sites*. The theory presented here suggests that the structural engineering to separate active sites (e.g., two Pt atoms) by inert elements (e.g., Au) is an effective approach for yielding a stable, active, and economic catalyst. Experimental observations on Au/Pt composite catalysts are discussed in the context of current findings, focusing on the thermodynamic tendency for AuPt surface alloy formation.

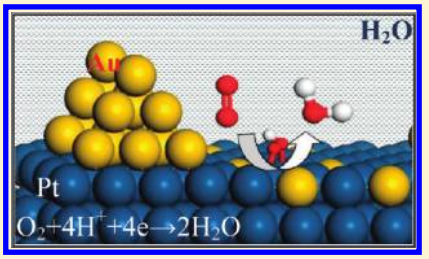

1. INTRODUCTION

How to efficiently reduce oxygen to water ($O_2 + 4H^+ + 4e \rightarrow 2H_2O$) is a major concern in fuel cell technology. For the traditional Pt cathode, it can catalyze the oxygen reduction reaction only below ~0.85 V vs NHE, i.e., with an overpotential of ~0.4 V.[1,2] Above 0.85 V, the surface oxidation and corrosion start to occur as dictated by thermodynamics, which is accompanied by the rapid decrease of activity.[3,4] To find better cathode material with both long-term stability and higher activity is however not trivial. In particular, the catalyst stability under the high potentials (>1 V) and acidic conditions appears to be a general problem, even for noble metals, such as Pt[3,5] and most Pt alloys.[6−8] For instance, Pd−Pt bimetallic nanodendrites were reported to exhibit a high activity for the oxygen reduction reaction (ORR) but show a loss of 30% active surface area after 4000 cycles of potential sweeps between 0.6 and 1.1 V.[6] To date, a deep understanding of the catalyst surface phase, the active site, and the reaction mechanism at the ORR working conditions is highly desired for finding a rational way to systematically improve both the stability and activity.

Because gold has a higher oxidation potential than Pt, the combination of Au with Pt was naturally anticipated to be a possible solution for producing a more stable cathode. The early experimental attempt by utilizing AuPt alloys as an ORR catalyst however failed to yield a qualified catalyst, as the ORR activity in acid medium was found to be dramatically quenched after AuPt bulk alloying.[9,10] This was attributed to the fact that Au has much poorer ORR activity than Pt (pure Au has a very high overpotential for ORR, >0.7 V). On the other hand, the recent experiment by Zhang et al.[11] pointed out a promising direction for stabilizing the Pt electrode. They deposited Au directly onto the Pt/carbon catalyst, in which the Au forms nanoparticles (2−3 nm) on the Pt surface. It was observed that this composite Au/Pt catalyst can achieve both a high stability and a comparable ORR activity with pure Pt.[12] The microscopic mechanism behind the stability and the activity of the Au/Pt composite catalyst

Received: June 8, 2011
Revised: August 1, 2011
Published: August 03, 2011

dx.doi.org/10.1021/jp205376b | J. Phys. Chem. C 2011, 115, 17508–17515

remains far from clear, however, not least because of the complex nature of the solid/liquid interface under electrochemical conditions.

For the ORR on pure Pt, great advances have been made recently, and the importance of Pt terrace sites was highlighted.[13−20] It was showed that the Pt(111) surface is prone to surface oxidation and corrosion at high potentials,[3,21−23] and (100)-facet dominated Pt nanoparticles can be synthesized by preferentially removing the (111) terrace under extensive potential cycling treatment.[24] To protect the (111) surface under high potentials is thus the key for stabilizing the Pt catalyst. As for the activity, Pt(111) was also inferred to contribute majorly to the ORR activity as the reaction is found to be not sensitive to the density of stepped sites in Pt nanoparticles[25] and the ORR activity drops by 1 order of magnitude from bulk to nanoparticle (∼2 nm) surfaces.[26−28] Despite the progress on pure Pt, the microscopic understanding of the corrosion process and the active site structure still falls much short of expectation and is not sufficient to rationalize the findings in the new AuPt composite system. It is puzzling, for example, why the addition of the chemically inert Au can improve the anticorrosion ability of the Pt catalyst dramatically without sacrificing the activity.[11,12] While one may expect that the high stability of the Au/Pt catalyst is related to the stabilization of the (111) terrace sites by Au, it is not clear why the Pt sites, especially those far away from the Au particle, can be stabilized considering that the Au particles only cover partially the Pt surface.[11] For the same reason, the area of active sites (exposed Pt) is expected to be much reduced, and the overall activity should decrease, apparently also in contradiction to the experimental observation.[11]

Considering that gold is chemically much more inert compared to Pt, the modification of Pt using Au provides a unique way to block, to separate, and even to heal the terrace and defected sites[23,29] of the Pt surface. This should enable us to identify the critical conditions required for the surface corrosion and the ORR to occur, which is the key step toward the rational design of a new ORR catalyst with both high activity and high stability. To this end, here we utilize Au to probe the activity and the stability of the Pt catalyst by correlating quantitatively the stability and the activity of the Au/Pt systems with the morphology/concentration of the added Au. A set of Au-modified Pt model systems under electrochemical conditions are investigated, including small Au clusters on the Pt surface and AuPt surface alloys by using the recently developed theoretical approach for electrocatalysis that integrates periodic density functional theory (DFT) calculations with a continuum solvation model.[30−32] We show that the presence of a very low amount of Au in the Pt surface layer can already protect the Pt surface from surface oxidation/corrosion while retaining the activity of Pt sites, which is attributed to the marked reduction in O coverage. In contrast, on the pure Pt surface a majority of surface Pt sites are in fact nonactive spectators, being terminated by oxidative species. We predict that the separation of active sites (e.g., Pt) by inert elements (e.g., Au) is a promising solution for obtaining a stable, active, and economic ORR catalyst.

2. CALCULATION METHODS

All DFT calculations were performed using the SIESTA package with numerical atomic orbital basis sets and Troullier−Martins norm-conserving pesudopotentials.[33−35] The exchange-correlation functional utilized was at the generalized gradient approximation level, known as GGA-PBE.[36] A double-ξ plus polarization basis (DZP) set was employed. The orbital-confining cutoff was determined from an energy shift of 0.010 eV. The energy cutoff for the real space grid used to represent the density was set as 150 Ry. The Quasi-Newton Broyden method was employed for geometry relaxation until the maximal forces on each relaxed atom were less than 0.1 eV/Å. To correct the zero-point energy (ZPE), the vibrational frequency calculations were performed via the finite-difference approach. Transition states (TSs) of the catalytic reaction were searched using the Constrained-Broyden-Minimization[37] and Constrained-Broyden-dimer method[38] developed recently. The ORR at the solid/liquid interface has been modeled using a periodic continuum solvation model based on the modified Poisson−Boltzmann equation (CM-MPB) to take into account the long-range electrostatic interaction due to solvation. The periodic DFT/CM-MPB method has been utilized in our previous work on electro-/photocatalysis, and details of the implementation are described therein.[30−32]

For the calculation of the surface phase diagram, we utilized p(4 × 4) and p(4 × 2$\sqrt{3}$) five-layer slabs for the Au/Pt systems with the top two Pt surface layers relaxed. A thicker six-layer slab with the top three layers relaxed was also utilized to compute more accurately the corrosion energetics involving the exposure of the subsurface Pt atoms (the effective slab thickness below the exposed atom is still five-layer). For ORR reaction on the Au cluster supported on Pt(111), an enlarged unit cell (p(5 × 2$\sqrt{3}$)) was used to calculate the reaction profile to minimize the possible lateral interaction due to the image of Au clusters. The Monkhorst−Pack type of k-point sampling with a (2 × 2 × 1) mesh was used in all calculations, and the denser (4 × 4 × 1) k-point mesh was used to further check the convergence of reaction energetics. The accuracy of the calculated energetics was examined by benchmarking the results from SIESTA with those from the plane-wave methodology. For example, the O_2 free energy of adsorption ($G(O_2)$) (with reference to the free energy of the gas-phase O_2 at the standard state) at 1/16 ML on Pt(111) is calculated to be 0.85 eV from SIESTA, and it is 0.86 eV from the plane-wave method.

To derive the free energy reaction profile, we first obtain the reaction energy of each step (strictly speaking, Helmholtz free energy change (ΔF) at 0 K, 0 bar) that is directly available from DFT total energy (ΔE) after the ZPE correction. For elementary surface reactions without involving the adsorption/desorption of gaseous or liquid molecules, ΔF at 0 K, 0 bar is a good approximation to the Gibbs free energy (ΔG) as the temperature T and pressure p contributions at the solid phase are small. To compute the free energy change ΔG of elementary reactions involving gaseous or liquid molecules, such as oxygen, hydrogen, and water, the large entropy term at 298 K is essential to take into account. We utilize the standard thermodynamic data[39] to obtain the temperature and pressure contributions for the G of the aqueous H_2O and gaseous H_2, which are −0.57 eV (the entropy contribution is −0.22 eV in solution) and −0.31 eV compared to the total energy of the corresponding free molecule (E, 0 K), respectively.[40] The G of O_2 is derived as $G[O_2] = 4.92$ (eV) + $2G[H_2O] - 2G[H_2]$ by utilizing OER equilibrium at the standard conditions. For reactions involving the release of the proton and electron, the reaction free energy can be computed by referencing to NHE as suggested by Bockris and Nørskov groups.[41,42] This is governed by $G_{proton+electron} = G_{1/2H2(g)} - eU$ where U is the electrochemical potential vs NHE.

3. RESULTS

3.1. Thermodynamics on the Surface Stability of Au/Pt Systems. *Surface Phase Diagram.* In this work, we have

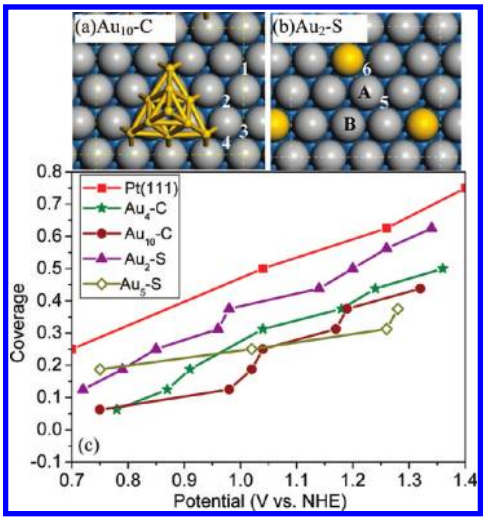

Figure 1. Two representative Au/Pt models (a and b) and the surface O coverage (c) of the Au/Pt systems at varied electrochemical potentials. Large gray ball: surface Pt. Large blue ball: subsurface Pt. Yellow ball: Au.

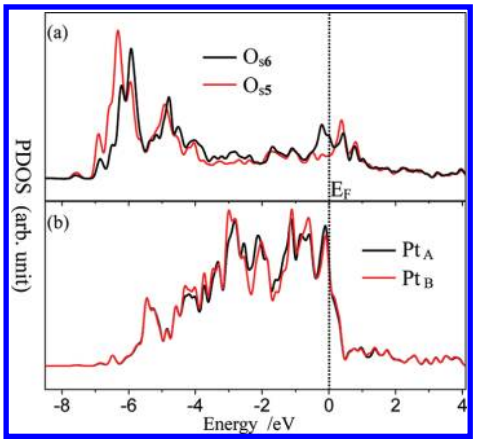

Figure 2. Projected density of states onto (a) the 2p states of adsorbed O atoms at the s**5** (Pt-only hollow site) and s**6** (PtPtAu hollow site) and (b) the 5d states of surface Pt_A and Pt_B of Au_2−S as indicated in Figure 1b.

considered two possible forms of Au on Pt, namely, Au particles on top of the Pt surface and the embedded Au atoms inside the Pt surface layer (surface alloy) (the structure for the Au/Pt composite catalyst is not known exactly from experiment[11]). Specifically, we investigated mainly four such systems, Au_4 and Au_{10} on Pt(111), both in three-dimensional pyramidal shape, denoted as Au_4−C and Au_{10}−C, respectively, and the AuPt surface alloys with 2:14 and 5:11 for the Au:Pt ratio at the surface layer, denoted as Au_2−S and Au_5−S, respectively. As the representative, the structures for Au_{10}−C and Au_2−S are illustrated in Figure 1a and b (the others are shown in the Supporting Information S-Figure 1). By examining these different AuPt models, we aim to gather a general overview on the Au-induced effects that are in common in different models and further identify the key quantities dictating the stability and the activity of ORR catalysts.

To evaluate the stability of these Au/Pt systems at high potential conditions, we need to first know the phase of the surface in contact with water at different potentials. We have constructed the phase diagram of the surfaces by correlating the surface O coverage with the applied electrochemical potential.[23,31,43] It is known that the coverage of O (from H_2O dissociation, $H_2O \rightarrow O + 2H^+ + 2e^-$) is sensitive to the applied potential: the coverage of the adsorbed O will increase with the elevation of the potential, which will eventually lead to the surface oxidation and corrosion. The coverage of O is critical to the kinetics of surface corrosion. The calculated O coverage for the Au/Pt model systems is shown in Figure 1c, where the results on pure Pt(111)[23] are also shown for comparison.

In calculating the surface phase diagram, we found that the adsorption of O obeys two general rules: (i) it adsorbs preferentially on the Pt sites of the (111) surface, and (ii) it prefers to adsorb at the Pt sites away from the Au. The presence of Au poisons the neighboring Pt sites for O adsorption. These can be understood as the Au being saturated in its d-states has a poorer covalent binding ability for O compared to Pt. As a result, the Au/Pt systems have a lower O coverage in general at the concerned ORR potentials (below 1.2 V) as shown in Figure 1c, although the morphology/concentration of the Au will also influence the O coverage. For example, below 1.0 V, the O coverage is only ~0.1 ML on Au_{10}-C/Pt, whereas it is up to ~0.5 ML on Pt(111).

It should be emphasized that the Au-induced destabilization effect to the adsorbed O atom drops rapidly as the distance between the Au and the adsorption site of O increases. For the Au_{10}−C system, for example, the calculated O atom adsorption free energies are −0.94, −0.68, −0.49, and 0.09 eV (1/16 ML) at the sites **1**−**4** (labeled in Figure 1a) from the farthest to the nearest according to their distance from the Au. At site **1** that is only about two lattices away from the Au cluster, the adsorption free energy is already close to the −1.03 eV on pure Pt(111). A similar phenomenon is also present in surface alloys. From the Au_2−S system, we can see that each Au atom in the surface can maximally passivate three neighboring fcc sites (**6** in Figure 1b). The calculated O atom adsorption free energies are −0.54 eV at the AuPtPt three-center hollow sites (site **6**, s**6**), while it is −1.01 eV on the Pt-only sites (site **5**, s**5**). These results indicate that the Au-induced change in the electronic structure of the surface is rather local, e.g., within a range of two lattice constants.

To provide more insight into the bonding of O on the Au-modified Pt surfaces, we have plotted in Figure 2 the calculated density of states projected (PDOS) onto the 2p states of the O atom adsorbed at s**5** and s**6** of Au_2−S and onto the 5d states of the surface Pt atoms with (Pt_A) and without (Pt_B) Au as the nearest neighbor (also see Figure 1b). It shows that the major difference in 2p(O) PDOS lies at −7 ~ −6 eV and 0−1 eV, which are the major bonding and antibonding states for O 2p bonding with Pt 5d states, respectively. For the O atom at the s**6** where a direct O−Au bond is present, the O 2p states are less stable (the bonding states shifting toward the high-energy regime) compared to those at the s**5** where only O−Pt bondings are involved. On the other hand, 5d(Pt) PDOS of Pt_A and Pt_B are very similar, indicating that Au does not change significantly the intrinsic bonding ability of Pt. These electronic structure analyses explain the local bonding picture of O adsorption, i.e., the rapid decay of Au-induced destabilization on O adsorption.

Surface Stability at High Potentials. Knowing the surface phase diagram, we can then investigate the stability of the systems at the high potentials.[43] From thermodynamics, the corrosion process is governed by the free energy change ΔG of the overall reaction formula 1 under electrochemical potentials, where O_x/Pt_s and $O_x - \square/Pt_s$ represent the phases before (O atoms on the surface) and after the corrosion. The surface phase after the

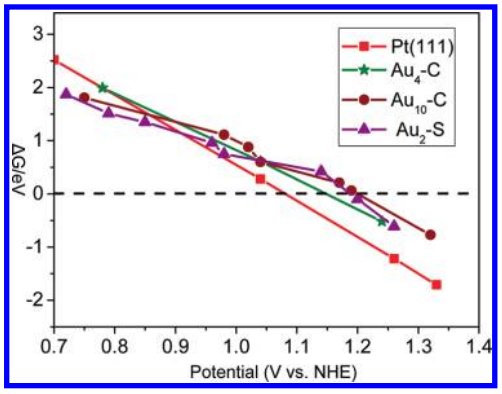

Figure 3. Calculated corrosion energy of the Au/Pt systems at different electrochemical potentials.

corrosion features a surface vacancy due to the dissolution of a surface Pt atom. It might be mentioned that reaction 1 describes the thermodynamic tendency of surface corrosion and should not be regarded as an elementary reaction step. For instance, the subsurface O may well be present before the Pt atom dissolution in the kinetic process of surface corrosion, and the penetration of surface O into the subsurface was shown to be assisted by the high local O coverage.[23]

$$O_x/Pt_s \rightarrow O_x - \square/Pt^{2+} + 2e^- \quad (1)$$

The ΔG of reaction 1 can be quantitatively evaluated with DFT. We utilize the standard thermodynamics data of the electrochemical half-cell reaction $Pt^{2+} + 2e^- \leftrightarrow Pt(s)$ (the equilibrium potential is 1.2 V at the standard condition) to derive the free energy for Pt^{2+} and electrons, i.e., $G(Pt^{2+} + 2e^-)|_{1.2V} = G(Pt)|_{1.2V}$. Considering that $G(Pt)$ of the Pt metal equals approximately the total energy of bulk Pt, $E_{coh}(Pt)$, $G(Pt^{2+} + 2e^-)$ at any potential U can be derived by computing $G(Pt^{2+} + 2e^-) = E_{coh}(Pt) - 2(U - 1.2)$, where the $2(U - 1.2)$ term accounts for the (de)stabilization of two electrons by the potential shift. Finally, the corrosion energy ΔG is derived as $\Delta G = E_{coh}(Pt) - 2(U - 1.2) + E(O_x - \square/Pt_s) - E(O_x/Pt_s)$, where the DFT total energy for the solid phases is utilized as an approximation to the total free energy. This approach has been utilized previously to evaluate the corrosion thermodynamics of pure Pt surfaces[23] and PtM skin alloys.[7]

The most stable surface vacancy phase, $O_x - \square/Pt_s$, for the Au_4−C, Au_{10}−C, and Au_2−S systems has been determined (all structures are shown in the Supporting Information S-Figure 2−3), and the calculated ΔG's of reaction 1 vs U are thus plotted in Figure 3. The data for pure Pt(111) are also plotted for comparison.[23] We found that the ΔG vs U curves for the three Au/Pt model systems are similar, which deviates from that of the pure Pt at the high potentials (above 1 V). For pure Pt, above 1.1 V, ΔG is already below zero, indicating a thermodynamic tendency toward the dissolution of surface Pt atoms. By contrast, ΔG of the Au/Pt systems remains positive (about 0.5 eV) until ∼1.2 V. This confirms that the presence of Au can retard the corrosion of the Pt surface. By comparing the two types of Au models, Au cluster and AuPt surface alloy, we can see from Figure 3 that the Au in the surface alloy is obviously more effective in stabilizing the Pt surface in terms of the amount of Au utilized. In Figure 4, we also highlight the structures for the Au_{10}−C/Pt and Au_2−S/Pt systems before and after the surface vacancy formation

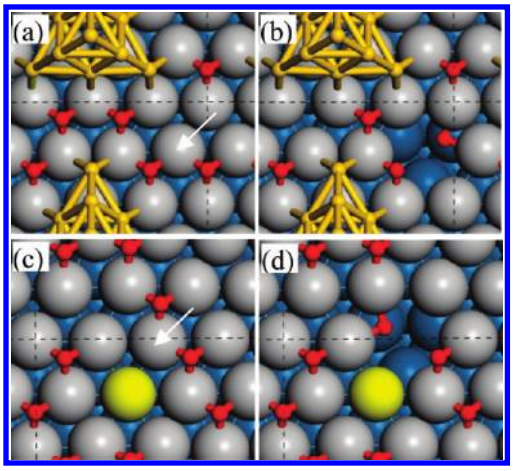

Figure 4. Optimized structures before (left) and after (right) the surface vacancy creation in Au_{10}−C (a and b) and Au_2−S (c and d) systems at ∼1.2 V, corresponding to 0.375 ML O in Au_{10}−C and 0.44 ML O in Au_2−S systems.

at ∼1.2 V, which is the most relevant to the surface corrosion (when ΔG becomes negative). It can be seen that the surface vacancy occurs generally at the Pt site with a high local O coverage at the initial state (IS), as indicated by the arrow in Figure 4. In this way, the surface vacancy can be maximally stabilized, where the preadsorbed O atoms sink into the second layer (subsurface O) to recover the bonding left by the leaving Pt atom.

It is natural to ask what the lowest O coverage is to initiate the Pt surface corrosion. By analyzing the surface vacancy phases with the increase of potential, we found that the critical local O coverage is 0.5 ML for both pure Pt(111) and the Au/Pt systems, in which every surface Pt atom must bond with two adsorbed O atoms. For the Au/Pt systems, as the O adsorption is highly heterogeneous, it is the sites distal to the Au that are preferentially populated by O and thus approach to local 0.5 ML first. On these sites, a local 0.5 ML O coverage is more difficult to achieve (shifting toward higher potential) compared to pure Pt, and thus the dissolution of Pt is hindered. In the Au_{10}−C system, for example, a 0.375 ML O coverage corresponds to a local coverage of 0.5 ML at the sites distal to Au (see Figure 4). Above this coverage, the calculated ΔG goes from positive to negative. Since the emergence potential of the 0.375 ML O coverage in the Au_{10}−C/Pt system is 1.19 V, being 0.15 V higher than that for 0.5 ML O coverage on pure Pt(111), the system exhibits a better anticorrosion ability than pure Pt. Similarly, the critical coverage for the Au_2−S surface alloy system is 0.44 ML O occurring at 1.14 V, and only above this coverage/potential, the corrosion becomes thermodynamically favorable. These results indicate that the local oxygen coverage is a key parameter to determine the surface corrosion tendency. The reduction in the O atom adsorption energy and thus the coverage can potentially improve the surface anticorrosion ability.

3.2. Oxygen Reduction on the Au/Pt Model Systems. We are now at the position to examine the ORR activity on these Au/Pt composite systems. Although there is no consensus on the exact ORR mechanism,[44−46] it was generally believed that two competing reaction pathways are present in ORR. The ORR is initiated by the molecular O_2 adsorption on the surfaces. Next, the adsorbed O_2 can either hydrogenate into OOH ($O_2^* + H^+ + e^- \rightarrow OOH^*$), denoted as the OOH pathway, which will

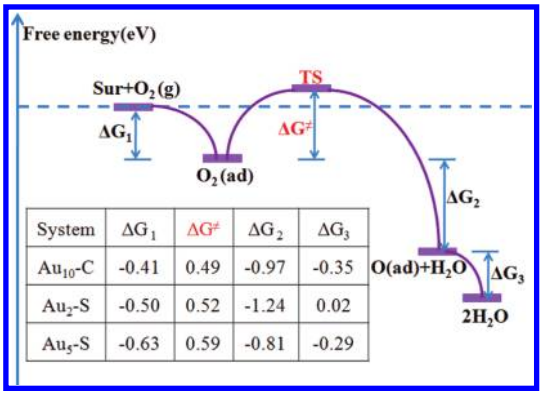

System	ΔG_1	$\Delta G^{\neq}$	ΔG_2	ΔG_3
Au_{10}-C	-0.41	0.49	-0.97	-0.35
Au_2-S	-0.50	0.52	-1.24	0.02
Au_5-S	-0.63	0.59	-0.81	-0.29

Figure 5. Simplified free energy profile for ORR on Au_{10}−C, Au_2−S, and Au_5−S systems at 0.8 V. The calculated values (eV) for ΔG_1, $\Delta G^{\ddagger}$, ΔG_2, and ΔG_3 are listed in the table. The solvation free energy of all states has been included by using the periodic continuum solvation model.[30−32]

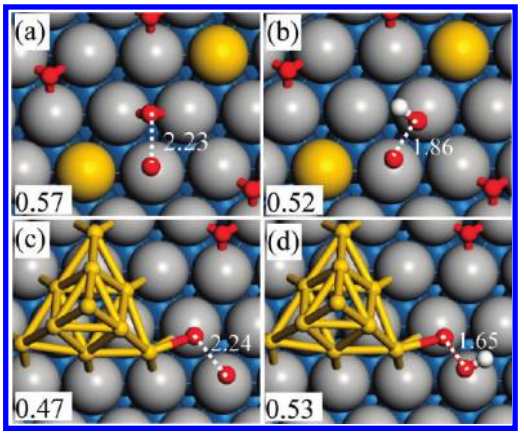

Figure 6. Located TS structures for O_2 (left) and OOH (right) dissociation at 0.8 V on the Au_2−S (a and b) and Au_{10}−C (c and d) systems with the O−O distance (in Å) labeled. The overall free energy barrier corresponding to the TS (in eV) is also indicated in the figure.

dissociate later into O and OH, or undergo a direct O−O splitting into atomic O, denoted as the O_2 dissociation pathway. No matter which reaction channel is followed, the final steps are the hydrogenation of O and OH into H_2O.[47−49] The elementary steps to break the O−O bond in both pathways on Pt(111) were found to be activated and believed to be the rate-determining step. Following this reaction mechanism, we can simplify the whole process into three key stages, namely: (i) O_2 adsorption stage (O_2 + sur → O_2*, ΔG_1); (ii) the adsorbed O atom stage (O_2* + $2H^+$ + $2e^-$ → H_2O + O*, ΔG_2); and (iii) the stage of the regenerated surface (O* + $2H^+$ + $2e^-$ → H_2O, ΔG_3). The O−O bond breaking occurs in between stages (i) and (ii), and the overall free energy barrier ($\Delta G^{\ddagger}$) can be computed by measuring the free energy difference between the stage (i) and the lowest-energy transition states (TS), either the OOH dissociation or the O_2 dissociation.

We have computed the free energy profile for ORR on Au_{10}−C, Au_2−S, and Au_5−S systems at 0.8 V, focusing on the free energy of the three key stages. The results are summarized in Figure 5, in which the energetic data for the lowest-energy reaction channel are tabulated, and the located TSs for the O−O bond breaking in the Au_{10}−C and Au_2−S systems are illustrated in Figure 6. The ISs for ORR are taken as the O-precovered surfaces, which are at 0.06, 0.19, and 0.19 ML O coverage for Au_{10}−C, Au_2−S, and Au_5−S systems, respectively, as determined from the surface phase diagram. It should be mentioned that the utilization of a realistic O precovered surface as the initial surface structure, instead of a clean surface, is essential for comparing the ORR activity between different systems since a small change in O coverage may influence the reaction energetics dramatically.

Despite the large difference in the morphology/concentration of Au, a common feature of the free energy profile is that the $\Delta G^{\ddagger}$ values of ORR for the Au/Pt systems are close, being 0.5−0.6 eV, which are also similar to those reported previously on the pure Pt(111) surface using the same theoretical approach.[7] This may not be too surprising as we found that the presence of a surface Au does not modify strongly the intrinsic bonding ability of Pt where ORR occurs, as indicated by the similar PDOS of 5d(Pt) shown in Figure 2b. In other words, the adsorption energy of key reaction intermediates that adsorb on the atop sites of Pt, such as O_2 and OOH, is not very sensitive to the presence of Au. Taking molecular O_2 adsorption as the example that sits on two atop sites of Pt at the IS (no direct bonding with Au), the calculated ΔG_1 is 0.41−0.63 eV on the Au/Pt systems at 0.8 V, in comparison with 0.5 eV on pure Pt(111).[7] The free energy barrier $\Delta G^{\ddagger}$, being the energy difference of the O_2 adsorption state and the TS for the dissociation O_2 or OOH, is therefore rather constant upon the addition of Au.

As for the concern of the overall reaction rate r that is a function of both the free energy barrier $\Delta G^{\ddagger}$ and the active site concentration θ (i.e., $r = A \exp(-\Delta G^{\ddagger}/RT)\theta$), we found that the presence of Au in fact does not necessarily reduce the active site concentration on the Pt surface. Apparently, this is because a substantial amount of preadsorbed O atoms (~0.25 ML) are present on pure Pt(111) above 0.8 V, while the O coverage is much reduced in Au/Pt systems at the same potentials. In the Au/Pt models investigated, we found that the concentration of the available reaction site is in fact rather similar, i.e., one reaction site per 16 Pt atoms (the active site is outlined in Supporting Information S-Figure 4).

The detailed ORR pathways in these systems are elaborated in the following. The ORR pathways on Au_2−S are similar to those identified on pure Pt(111).[7,16] Both the O_2 dissociation and the OOH pathways are present at 0.8 V, and the calculated $\Delta G^{\ddagger}$ for the two pathways are 0.57 and 0.52 eV, respectively (see Figure 6). In the O_2 dissociation pathway, the O−O bond breaking occurs over a free Pt triangle involving three Pt atoms at the TS, while the OOH dissociation needs only two Pt atoms (Figure 6a and b). The ORR on Au_{10}−C is perhaps of more interest, as it occurs at the interface between the Au cluster and the Pt surface. At the IS, O_2 adsorbs at two Pt atop sites with one O forming an additional O−Au bond with the neighboring Au cluster. On going from the IS to the TS of O_2 dissociation (Figure 6c), the O−Au distance shortens from 2.33 to 2.16 Å, indicating that the Au cluster can help to stabilize the TS. The TS for OOH dissociation (Figure 6d) is similar to that of O_2 dissociation but with a slightly higher $\Delta G^{\ddagger}$ at 0.8 V. Since the $\Delta G^{\ddagger}$ values for the two reaction pathways at 0.8 V are generally close (within 0.1 eV) in these Au/Pt systems, it is expected that dual reaction channels are present in ORR, and the contribution of each channel on the overall rate should depend on the exact reaction conditions, e.g., the applied potential.

By comparing the identified ORR pathway on the Au/Pt systems, we found interestingly that the increase of Au concentration in the Pt surface alloy (from Au_2−S to Au_5−S) does not

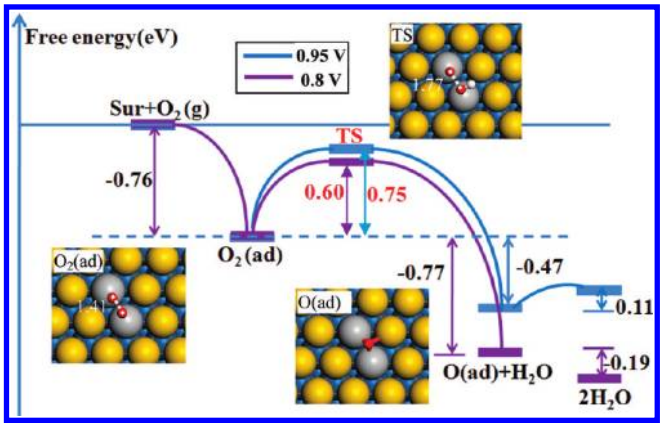

Figure 7. Simplified free energy profile for ORR on Au_{14}−S systems at 0.8 V (purple line) and 0.95 V (blue line).

deteriorate/increase the ORR activity obviously. This implies that the active site of Pt for ORR is not much affected by the increase of Au. Therefore, it is of interest to examine the ORR activity on the AuPt surface alloy with a maximum Au concentration. At such an extreme condition, not only can the Pt utilization be maximally reduced but also the Pt corrosion should be quenched due to the reduced local coverage of O atoms at high potentials. By increasing the Au concentration to 7/8 ML (Au_{14}−S) in the AuPt surface alloy (only two neighboring Pt atoms are available per unit cell), as shown in Figure 7, we investigated the surface phase diagram, the surface stability, and the ORR activity of the Au_{14}−S system using the same approach described above. In this AuPt model system, the Pt sites are well separated by Au atoms, and the two Pt atoms as one active site are just enough for ORR via the OOH pathway. Due to the high concentration of Au and the poor adsorption free energy of the O atom on this surface (−0.67 eV at 1/16 ML), we found that, not surprisingly, the O coverage on this surface is very low (<0.1 ML below 1.2 V, see Supporting Information S-Figure 5), and the surface is therefore anticorrosive below 1.2 V.

The ORR kinetics on the Au_{14}−S model system at 0.8 and 0.95 V are studied, and the simplified ORR free energy profiles are shown in Figure 7. On the surface, molecular O_2 can adsorb on the atop sites of two Pt atoms with the calculated adsorption free energy being 0.76 eV. Next, the O_2 reduction can undergo a hydrogenation process to OOH, followed by the dissociation of OOH to an adsorbed O atom and OH. The calculated free energy barriers are 0.60 eV at 0.8 V and 0.75 eV at 0.95 V, which are generally feasible for a reaction to occur at the ambient conditions. These results indicate that (i) ORR can occur facilely even at the high concentration of Au in the surface alloy and that the activity at 0.8 V is not very sensitive to the amount of Au in the surface layer (0.52, 0.59, and 0.60 eV for Au_2−S, Au_5−S, and Au_{14}−S systems) and that (ii) with a high concentration of Au, ORR can occur potentially at a higher potential (e.g., 0.95 V demonstrated here) because the O coverage is much reduced by the high concentration of Au and the reaction is not be poisoned by the precovered O.

Our results on the series of AuPt surface alloys demonstrate that only a small number of Pt sites on the (111) terrace take part in ORR at the concerned electrochemical potentials. On pure Pt, the dominant amount of Pt surface sites is in fact not catalytically active (e.g., 0.25 ML O coverage at 0.8 V and up to 0.5 ML at 1.05 V on Pt(111)) due to the termination of adsorbed O atoms. Since one active ORR site contains only two neighboring Pt atoms as identified in this work, ORR can occur without requiring the specific open surface structures that are unique to surface steps and can also tolerate a certain amount of O precoverage. This picture on the ORR reaction site can be used to rationalize important experimental findings; for example, the ORR activity is not sensitive to the density of stepped sites on Pt nanoparticles,[25] and the ORR activity decreases as the Pt particle size decreases.[26,27] These experimental findings suggest that it is the area of the (111) terrace, not the density of the steps, that is more important to ORR activity. Terraces, despite being covered by O atoms, still contain most exposed Pt atoms and thus contribute dominantly to ORR activity. To improve further ORR activity at high potentials, the O coverage must be reduced. A possible solution as suggested here by the Au_{14}−S system is to separate and minimize each active site that contains only two Pt atoms, which can significantly weaken the adsorption of O atoms but remains catalytically active for O_2 reduction via the OOH pathway.

4. GENERAL DISCUSSION ON THE AUPT SURFACE ALLOY

The most striking finding in this work is perhaps that the AuPt surface alloy with a low amount of Au in the Pt surface layer is already a stable material with a good ORR activity, and the Au clusters are in fact not essential. From our results, the amount of Au in the AuPt surface alloy can be as low as 1/8 ML. It is therefore interesting to ask whether the AuPt alloy is present in experiment, in addition to the observed Au nanoparticles.[11]

We have shown that the presence of Au particles on the surface can only prevent the corrosion of Pt sites that are close to the Au. It is expected that only finely dispersed Au clusters, such as the Au_{10}−C investigated in this work, can stabilize the whole surface and thus prevent the corrosion process. However, the experimentally prepared Au particles are not small (about 2−3 nm) and cover one-third of the Pt sites, indicating the strong sintering tendency of Au in the potential cycling experiment (in Zhang's experiment, the Au layer on Pt is shown to transform into three-dimensional clusters after undergoing several potential sweeps up to 1.2 V[11]). Since a great number of Pt surface sites that are more than two lattices away from the Au cluster remain unprotected, the Au nanoparticle model alone cannot explain satisfactorily the observed anticorrosion of the Au/Pt composite.

To better understand the Au morphology under the electrochemical treatment, we have carried out the following thermodynamic analysis to compare the relative stability of Au_4−C, Au_{10}−C, and Au_2−S systems. The phase change involving the three systems under the electrochemical conditions can be described by the following reactions 2 and 3, where x, y, and z represent the O coverage of the systems at the concerned electrochemical potentials. It is noted that the coverage of O, x, and y, on the Au/Pt systems, is always lower than that, z, in Pt(111).

$$2.5O_x/Au_4 - C + (1.5z + y - 2.5x)H_2O \rightarrow O_y/Au_{10} - C + 1.5O_z/Pt + (3z + 2y - 5x)(H^+ + e^-) \quad (2)$$

$$O_y/Au_{10} - C + 4O_z/Pt + (8z + 2y - 10x)(H^+ + e^-) \rightarrow 5O_x/Au_2 - S + 10Pt^{2+} + (4z + y - 5x)H_2O \quad (3)$$

As shown in Figure 8, by comparing first the stability of Au_4−C (green line) and Au_{10}−C (red line) model systems (reaction 2), we found that the Au_4−C is more stable than

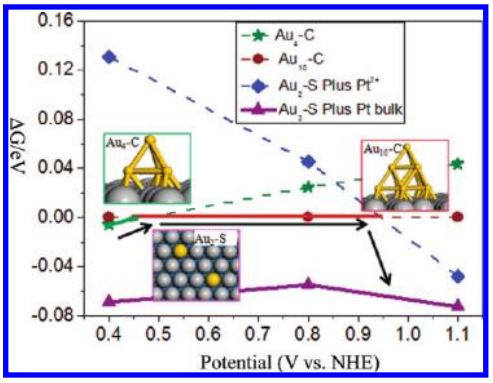

Figure 8. Relative stability (ΔG per site) of Au_4-C, $Au_{10}-C$, and Au_2-S at the potential regime from 0.4−1.1 V. The black arrow following the solid lines indicates the thermodynamic tendency to form the AuPt surface alloy.

$Au_{10}-C$ only below ~0.45 V, which is in accordance with the observation that Au particles tend to grow larger at elevated potentials. This is driven by thermodynamics to free more Pt surface sites for allowing the adsorption of more O atoms. Next, we compared the stability of the $Au_{10}-C$ system with the Au_2-S system by using reaction 3, where surface Pt atoms dissolve into the Pt^{2+} cation and the formed surface vacancy is then healed by Au to form the Au_2-S surface alloy. We found that above 0.95 V $Au_{10}-C$ becomes less stable than the Au_2-S surface alloy. It is noticed that the Pt^{2+} ions in solution can then be reduced to Pt metal back to the solid state, which is thermodynamically favorable below 1.2 V. Therefore, the AuPt surface alloys together with the deposited Pt metal island (purple line) are the thermodynamically most stable surface phase and may well be present after extensive potential cycling treatment.

On the basis of our results, we can rationalize the experimental findings as follows. During the potential cycling experiment, once a surface vacancy is created at the sites distal to the Au particles at the high potentials, the following low potential sweep will facilitate the surface Au diffusing to the surface vacancy, which heals the vacancy by forming the surface alloy. Such a process will continue until a certain critical concentration of Au in Pt is reached. As the newly formed AuPt surface alloy will increase the anticorrosion ability of the surface, the Au amount in the surface alloy will not be high, e.g., 1/8 ML, as shown in this work. The in situ formed AuPt surface alloy is the key for understanding the anticorrosion ability of the electrode.

Finally, we also would like to emphasize that the AuPt surface alloy performs distinctly as an ORR catalyst compared to the PtM skin alloys, such as Pt_3Ni[50] and Pt_3Co[51] catalysts (the first layer is Pt, and the layer underneath is PtM bulk alloys). The PtM skin alloys were reported to exhibit a higher ORR activity than pure Pt, while the AuPt surface alloy does not improve the ORR activity obviously. The enhanced activity in the PtM skin alloy was attributed to the reduced binding ability (e.g., O_2 and O) of the surface Pt due to the stabilization of surface Pt d states.[50,52] Unlike that in PtM skin alloys, the presence of Au does not modify strongly the intrinsic binding ability of Pt and thus has a little effect on the ORR activity. As for the surface stability, we recently found that most of the PtM skin alloys, especially M being 3d metal, are not more resistant to surface oxidation than pure Pt by examining the stability of a set of PtM skin alloys (M = 3d and 4d metals) at high potentials.[7] Despite that the surface O coverage in PtM skin alloys can be lower than pure Pt, the dissolution of surface Pt is thermodynamically favored even at a relatively low O coverage on PtM skin alloys due to the preference to form a stronger O−M ionic bonding at the subsurface. In contrast, the reduced O coverage in AuPt surface alloys is related directly to the weak O−Au bond that the adsorbed O tends to avoid. The dissolution of Pt is hindered in the AuPt surface by the low O coverage. Obviously, the overall effects on the activity and the stability for the AuPt surface alloy and the PtM skin alloys are just opposite, and the combination of the merits of the two distinct systems could be an interesting direction for the design of new ORR catalysts in the future.

5. CONCLUSION

By investigating the stability and the activity of a set of Au/Pt model systems using an integrated theoretical approach for electrocatalysis based on first-principles calculations and a periodic continuum solvation model, this work outlines some key factors dictating the catalytic performance of ORR on Pt. Since Au is catalytically much more inert than Pt in ORR, the detailed analysis on the Au-modified Pt systems enables us to shed insight into the catalytic behavior of Pt under ORR operating conditions, including those related to surface corrosion and ORR kinetics. The surface phase diagram, the corrosion thermodynamics, and the ORR kinetics of the Au/Pt composite systems under realistic electrochemical conditions are determined within a unified theoretical framework, which provides rich information on the microscopic mechanism of Pt surface corrosion and ORR kinetics. We propose that for achieving both high activity and high stability of ORR catalyst it is critical to separate and minimize the active site, which can reduce the O coverage without losing ORR activity even at high potentials. Our detailed results are summarized as follows.

A critical local O coverage of 0.5 ML is identified for initiating the corrosion of Pt surface sites, in which each Pt atom is at least bonded with two O atoms. The presence of Au can reduce the local O coverage at high potentials and thus stabilize the Pt surface. It is found that both Au clusters and the AuPt surface alloy can increase the anticorrosion ability of Pt up to 1.2 V. In terms of the amount of Au utilized, the AuPt surface alloy is much more effective to achieve a stable ORR catalyst, in which the Au concentration can be as low as 1/8 ML in the surface alloy.

Two neighboring Pt atoms on the surface are enough to catalyze ORR via a OOH pathway. On pure Pt, the majority surface Pt sites are in fact nonactive spectators that are terminated by O atoms at the working potentials, e.g., 0.25 ML O at 0.8 V. The presence of Au does not influence strongly the local bonding ability of Pt sites, and thus the ORR catalytic activity is retained after the addition of Au. By thermodynamics analysis of the Au/Pt model systems, we demonstrate that the AuPt surface alloy can be produced after the potential cycling treatment and is the key component responsible for the experimental observation on the Au/Pt composite.

■ ASSOCIATED CONTENT

Supporting Information. The structures for the Au_4-C and Au_5-S model systems; optimized structures on $Au_{10}-C$ systems before and after the surface vacancy creation from 0.7 to 1.2 V; optimized structures on Au_2-S systems before and after the surface vacancy creation from 0.7 to 1 V; the reaction site of

ORR on Pt(111), Au_{10}−C, Au_2−S, and Au_5−S systems at 0.8 V; the O coverage of the Au_{14}−S system at varied electrochemical potentials. This material is available free of charge via the Internet at http://pubs.acs.org.

AUTHOR INFORMATION

Corresponding Author
*Fax: (+86) 21-6564-2400. E-mail: zpliu@fudan.edu.cn.

ACKNOWLEDGMENT

This work is supported by NSF of China (20825311), 973 program (2011CB808500), Science and Technology Commission of Shanghai Municipality (08DZ2270500), and Program for Professor of Special Appointment (Eastern Scholar) at Shanghai Institute of Higher Learning.

REFERENCES

(1) Gasteiger, H. A.; Kocha, S. S.; Sompalli, B.; Wagner, F. T. *Appl. Catal. B: Environ.* **2005**, *56*, 9.
(2) Wang, C.; Daimon, H.; Onodera, T.; Koda, T.; Sun, S. H. *Angew. Chem., Int. Ed.* **2008**, *47*, 3588.
(3) Shao-Horn, Y.; Sheng, W. C.; Chen, S.; Ferreira, P. J.; Holby, E. F.; Morgan, D. *Top. Catal.* **2007**, *46*, 285.
(4) Conway, B. E. *Prog. Surf. Sci.* **1995**, *49*, 331.
(5) Dai, Y.; Ou, L. H.; Liang, W.; Yang, F.; Liu, Y. W.; Chen, S. L. *J. Phys. Chem. C* **2011**, *115*, 2162.
(6) Lim, B.; Jiang, M. J.; Camargo, P. H. C.; Cho, E. C.; Tao, J.; Lu, X. M.; Zhu, Y. M.; Xia, Y. A. *Science* **2009**, *324*, 1302.
(7) Wei, G. F.; Liu, Z. P. *Energy Environ. Sci.* **2011**, *4*, 1268.
(8) Greeley, J.; Norskov, J. K. *J. Phys. Chem. C* **2009**, *113*, 4932.
(9) Luo, J.; Njoki, P. N.; Lin, Y.; Wang, L. Y.; Zhong, C. J. *Electrochem. Commun.* **2006**, *8*, 581.
(10) Tang, W.; Jayaraman, S.; Jaramillo, T. F.; Stucky, G. D.; McFarland, E. W. *J. Phys. Chem. C* **2009**, *113*, 5014.
(11) Zhang, J.; Sasaki, K.; Sutter, E.; Adzic, R. R. *Science* **2007**, *315*, 220.
(12) Zhang, Y.; Huang, Q. H.; Zou, Z. Q.; Yang, J. F.; Vogel, W.; Yang, H. *J. Phys. Chem. C* **2010**, *114*, 6860.
(13) Kuzume, A.; Herrero, E.; Feliu, J. M. *J. Electroanal. Chem.* **2007**, *599*, 333.
(14) Markovic, N.; Gasteiger, H.; Ross, P. N. *J. Electrochem. Soc.* **1997**, *144*, 1591.
(15) Anderson, A. B.; Albu, T. V. *J. Am. Chem. Soc.* **1999**, *121*, 11855.
(16) Keith, J. A.; Jacob, T. *Angew. Chem., Int. Ed.* **2010**, *49*, 9521.
(17) Tripkovic, V.; Skulason, E.; Siahrostami, S.; Norskov, J. K.; Rossmeisl, J. *Electrochim. Acta* **2010**, *55*, 7975.
(18) Janik, M. J.; Taylor, C. D.; Neurock, M. *J. Electrochem. Soc.* **2009**, *156*, B126.
(19) Wang, J. X.; Markovic, N. M.; Adzic, R. R. *J. Phys. Chem. B* **2004**, *108*, 4127.
(20) Panchenko, A.; Koper, M. T. M.; Shubina, T. E.; Mitchell, S. J.; Roduner, E. *J. Electrochem. Soc.* **2004**, *151*, A2016.
(21) Imai, H.; Izumi, K.; Matsumoto, M.; Kubo, Y.; Kato, K.; Imai, Y. *J. Am. Chem. Soc.* **2009**, *131*, 6295.
(22) Jerkiewicz, G.; Vatankhah, G.; Lessard, J.; Soriaga, M. P.; Park, Y. S. *Electrochim. Acta* **2004**, *49*, 1451.
(23) Fang, Y. H.; Liu, Z. P. *J. Phys. Chem. C* **2010**, *114*, 4057.
(24) Tian, N.; Zhou, Z. Y.; Sun, S. G.; Ding, Y.; Wang, Z. L. *Science* **2007**, *316*, 732.
(25) Lee, S. W.; Chen, S.; Suntivich, J.; Sasaki, K.; Adzic, R. R.; Shao-Horn, Y. *J. Phys. Chem. Lett.* **2010**, *1*, 1316.
(26) Mayrhofer, K. J. J.; Strmcnik, D.; Blizanac, B. B.; Stamenkovic, V.; Arenz, M.; Markovic, N. M. *Electrochim. Acta* **2008**, *53*, 3181.
(27) Mayrhofer, K. J. J.; Blizanac, B. B.; Arenz, M.; Stamenkovic, V. R.; Ross, P. N.; Markovic, N. M. *J. Phys. Chem. B* **2005**, *109*, 14433.
(28) Greeley, J.; Rossmeisl, J.; Hellman, A.; Norskov, J. K. *Z. Phys. Chem.: Int. J. Res. Phys. Chem. Chem. Phys.* **2007**, *221*, 1209.
(29) Vang, R. T.; Honkala, K.; Dahl, S.; Vestergaard, E. K.; Schnadt, J.; Laegsgaard, E.; Clausen, B. S.; Norskov, J. K.; Besenbacher, F. *Nat. Mater.* **2005**, *4*, 160.
(30) Wang, H. F.; Liu, Z. P. *J. Phys. Chem. C* **2009**, *113*, 17502.
(31) Fang, Y. H.; Liu, Z. P. *J. Am. Chem. Soc.* **2010**, *132*, 18214.
(32) Li, Y. F.; Liu, Z. P.; Liu, L. L.; Gao, W. G. *J. Am. Chem. Soc.* **2010**, *132*, 13008. Shang, C.; Liu, Z.-P. *J. Am. Chem. Soc.* **2011**, *133*, 9938.
(33) Soler, J. M.; Artacho, E.; Gale, J. D.; Garcia, A.; Junquera, J.; Ordejon, P.; Sanchez-Portal, D. *J. Phys.: Condens. Matter* **2002**, *14*, 2745.
(34) Junquera, J.; Paz, O.; Sanchez-Portal, D.; Artacho, E. *Phys. Rev. B* **2001**, *64*, 235111.
(35) Troullier, N.; Martins, J. L. *Phys. Rev. B* **1991**, *43*, 1993.
(36) Perdew, J. P.; Burke, K.; Ernzerhof, M. *Phys. Rev. Lett.* **1996**, *77*, 3865.
(37) Wang, H. F.; Liu, Z. P. *J. Am. Chem. Soc.* **2008**, *130*, 10996.
(38) Shang, C.; Liu, Z. P. *J. Chem. Theory Comput.* **2010**, *6*, 1136.
(39) *CRC Handbook of Chemistry and Physics*, 84th ed.; R.LIDE, D., Ed.; CRC press: Boca Raton, FL, 2003−2004.
(40) Liu, Z. P.; Jenkins, S. J.; King, D. A. *J. Am. Chem. Soc.* **2004**, *126*, 10746.
(41) Bockris, J. O. M.; Khan, S. U. M. *Surface Electrochemistry*; Plenum Press: New York, 1993.
(42) Rossmeisl, J.; Logadottir, A.; Norskov, J. K. *Chem. Phys.* **2005**, *319*, 178.
(43) Fang, Y. H.; Liu, Z. P. *J. Phys. Chem. C* **2009**, *113*, 9765.
(44) Clouser, S. J.; Huang, J. C.; Yeager, E. *J. Appl. Electrochem.* **1993**, *23*, 597.
(45) Li, X.; Gewirth, A. A. *J. Am. Chem. Soc.* **2005**, *127*, 5252.
(46) Anderson, A. B.; Roques, J.; Mukerjee, S.; Murthi, V. S.; Markovic, N. M.; Stamenkovic, V. *J. Phys. Chem. B* **2005**, *109*, 1198.
(47) Jacob, T.; Goddard, W. A. *ChemPhysChem* **2006**, *7*, 992.
(48) Anderson, A. B.; Albu, T. V. *J. Electrochem. Soc.* **2000**, *147*, 4229.
(49) Norskov, J. K.; Rossmeisl, J.; Logadottir, A.; Lindqvist, L.; Kitchin, J. R.; Bligaard, T.; Jonsson, H. *J. Phys. Chem. B* **2004**, *108*, 17886.
(50) Stamenkovic, V. R.; Fowler, B.; Mun, B. S.; Wang, G. F.; Ross, P. N.; Lucas, C. A.; Markovic, N. M. *Science* **2007**, *315*, 493.
(51) Stamenkovic, V. R.; Mun, B. S.; Arenz, M.; Mayrhofer, K. J. J.; Lucas, C. A.; Wang, G. F.; Ross, P. N.; Markovic, N. M. *Nat. Mater.* **2007**, *6*, 241.
(52) Stamenkovic, V.; Mun, B. S.; Mayrhofer, K. J. J.; Ross, P. N.; Markovic, N. M.; Rossmeisl, J.; Greeley, J.; Norskov, J. K. *Angew. Chem., Int. Ed.* **2006**, *45*, 2897.